Journal of Catalysis 265 (2009) 229–237

Contents lists available at ScienceDirect

Journal of Catalysis

journal homepage: www.elsevier.com/locate/jcat

Heterogeneously catalyzed asymmetric hydrogenation of α-arylenamides over immobilized RhBPE and RhDUPHOS complexes

Adrian Crosman, Wolfgang F. Hoelderich *

Department of Chemical Technology and Heterogeneous Catalysis, University of RWTH-Aachen, Worringerweg 1, 52074 Aachen, Germany

ARTICLE INFO

Article history:
Received 7 January 2009
Revised 12 February 2009
Accepted 6 May 2009
Available online 31 May 2009

Keywords:
Hydrogenation
Enantioselectivity
Arylenamide
Ruthenium
Rhodium
Heterogeneous chiral catalysts

ABSTRACT

Optically active α-1-arylalkylamine derivatives were successfully synthesized through heterogeneous asymmetric hydrogenation of α-arylenamides over immobilized RhBPE and RhDUPHOS complexes on aluminum-containing M41S and SBA-15 type materials. The heterogeneous chiral catalysts were prepared by immobilization of rhodium diphosphine complexes on Al-MCM-41, Al-MCM-48, and Al-SBA-15. The complexes were bonded to the carrier by the interaction of the cationic rhodium of the organometallic complex with the anionic host framework, as well as between Al Lewis acid sites and P Lewis basic sites. The catalysts were characterized with XRD, FT-IR and MAS-NMR, as well as thermoprogramed desorption of ammonia, thermogravimetric analysis, and nitrogen sorption experiments. The immobilized catalysts showed high activities and excellent chemo- and enantioselectivities. Up to 99% e.e. at 99% conversion and >99% chemoselectivity were observed in the case of studied α-arylenamides. The catalysts could be reused up to four times without loss of catalytic activity or enantioselectivity.

1. Introduction

Optically active α-1-arylalkylamines constitute an important class of compounds that have been employed extensively as resolving agents, chiral auxiliaries, and intermediates in the synthesis of a wide range of biologically active molecules [1,2]. Many reliable synthetic methods have been described in the literature. Generally, these methods involve optical resolution procedures, biocatalytic methods, or stoichiometric use of chiral precursors or chiral auxiliaries [3–5]. Asymmetric catalytic reduction of C=N or C=C double bonds potentially could provide a very efficient and a convenient route to many chiral amine derivatives. Recently, success along these lines of research was achieved exclusively in homogeneous catalysis [6,7].

Homogeneous catalysts are known to exhibit high selectivity and activity in a variety of asymmetric transformations under relatively mild conditions. In 2001, the significant achievements in the design and application of asymmetric homogeneous catalysts were recognized by the award of the Chemistry Nobel Prize to Knowles and Noyori for enantioselective hydrogenation catalysis and to Sharpless for enantioselective oxidation catalysis [8–10]. However, despite the huge amount of work devoted to this subject in both academic and industrial fields, homogeneous asymmetric catalysis is most probably not used at its full extent in the overall production of chiral chemicals [11,12]. Due to the cost of sophisticated chiral ligands, often exceeding that of the noble metal employed, catalyst recovery is of paramount importance for the application of enantioselective metal catalysis to large-scale processes, eventually in continuous flow reactors. Furthermore, even if the activity and selectivity of homogeneous catalysts is exceptionally high, toxicological and environmental problems should also be taken into account.

Since the late 1960s, many approaches have been published by academia and industry to "heterogenize", "immobilize" or "anchor" a homogeneous catalyst [13–16]. In addition, many excellent reviews have emerged in the recent years, which describe in detail the synthesis and (academic) use of polymer-supported catalysts [17–27] and catalysts on inorganic carriers [28–32], or both [33–35]. Covalent binding is by far the most frequently used strategy. It can be effected either by copolymerization of functionalized ligands with a suitable monomer, or by grafting functionalized ligands or metal complexes with reactive groups on to a preformed support.

Another common and simple immobilization technique of catalytically active metal complexes is ionic binding, which is particularly useful for cationic rhodium or palladium catalysts. Various supports with ion-exchange capabilities can be used, including standard organic or inorganic ion-exchange resins, inorganic materials with polarized groups, and zeolites [28,29,32]. The advantage of immobilization by adsorption is the ease of preparation of the heterogenized catalyst by simple procedures, very often even without the need to previously functionalize the ligand. In this respect,

* Corresponding author. Fax: +49 241 8022291.
E-mail address: hoelderich@rwth-aachen.de (W.F. Hoelderich).

0021-9517/$ - see front matter © 2009 Elsevier Inc. All rights reserved.
doi:10.1016/j.jcat.2009.05.006

immobilization by ionic binding can be seen as a special case of heterogenization via adsorption [36,37].

Using entrapment as a method for heterogenization, the size of the metal complex is more important than the specific adsorptive interaction. There are two different preparation strategies: One is based on building up catalysts in well-defined cages of porous supports. This approach is also called "ship in a bottle" [38]. The other approach is to build up a polymer network around a preformed catalyst.

Supported aqueous-phase catalysts (SAPCs) can be seen as a special case of adsorption, whereby a water-soluble catalyst dissolved in a very polar solvent is adsorbed on a hydrophilic support forming a water film on the inner surface of the support [39,40]. In the case of supported liquid-phase catalysis (SLPC), the water film on the inner surface is replaced by a solvent of low vapor pressure (e.g., phthalic acid esters) [41]. The reaction itself takes place in the supported liquid or at the interface of the supported liquid film, or in the gas phase or organic phase when dealing with SLPC or SAPC, respectively. The use of SLPC catalysts is generally restricted to the synthesis of low-boiling compounds.

Mesoporous molecular sieves have received much attention in the field of catalysis, especially for their use as supports. Our group has previously reported the successful immobilization of different homogeneous catalysts on such molecular sieves (e.g., Al-MCM-41, Al-MCM-48, and Al-SBA-15) and their use in asymmetric hydrogenation, epoxidation, and ring opening of epoxides [42–45]. Recently, Hutchings et al. reported the immobilization of RhDuphos on Al-MCM-41 and its use for asymmetric hydrogenation of dimethyl itaconate and methyl-2-acetamidoacrylate [46]. Herein, we present a novel method for the synthesis of optically active α-1-arylalkylamines derivatives through asymmetric hydrogenation of α-arylenamides over immobilized RhBPE and RhDUPHOS complexes on mesoporous materials. Ion exchange, catalytic, and adsorptive properties of molecular sieve materials are based on the existence of acid sites which arise from the presence of accessible hydroxyl groups associated with tetrahedral aluminum in the silica–alumina framework. Our research was focused on the use of M41S and SBA-15 type materials as carriers, which are characterized by a well-defined pore structure and high surface area, offering new opportunities for the immobilization of large homogeneous catalyst species without any modification of their chemical structure. The heterogenization is based on an ionic interaction between the negatively charged Al-M41S or Al-SBA-15 framework and the cationic rhodium of the organometallic complex. Furthermore, activity of the obtained catalysts was investigated in the enantioselective hydrogenation of different α-1-arylalkylenamides.

2. Experimental

It is well known that Rh-complexes containing diphosphines are very sensitive to moisture and oxygen. Phosphines can be easily oxidized under such conditions, and then lose their catalytic activity. Considering these reasons, all the experiments involving diphosphines, rhodium diphosphine complexes, and immobilized complexes were carried out in argon-filled MBRAUN LabStar glovebox or using standard Schlenk-type techniques. In order to remove all adsorbed water molecules, the solid supports were calcined overnight at 300 °C prior to the immobilization of organometallic complexes. Moreover, all used solvents were dried and degassed using well-known standard methods.

2.1. Preparation of the mesostructured materials

Al-MCM-41 was prepared according to a slightly altered method reported by van Hooff [47]. In a 250 mL PE flask, 10.5 g tetraethylammonium hydroxide (TEAOH, 40 wt.%, aqueous), 0.21 g $NaAlO_2$, and 50 g H_2O were mixed together and stirred at room temperature for 1 h, followed by the addition of 10 g tetradecyltrimethylammonium bromide. The resulting mixture was stirred for 4 h. Then, 15.23 g Ludox-HS 40 was added dropwise over a period of 1 h, followed by vigorous stirring at ambient temperature for 4 h. The crystallization took place at 105 °C for 6 days. After the third and fifth day, pH was adjusted at 10.2 using CH_3COOH (10 wt.%, aqueous). After crystallization, the solid phase was recovered by filtration and washed well with water. The white material was dried at 120 °C overnight, followed by calcination in static air at 540 °C for 6 h (heating rate 1 °C/min).

Al-MCM-48 was prepared as follows: in a 500 mL PE flask, TEAOH (40 wt. %, aqueous), $NaAlO_2$, and water were stirred at room temperature for 1 h, followed by the addition of cetyltrimethylammonium bromide. Then, Ludox HS-40 was added dropwise over a period of 1 h, followed by vigorous stirring for 4 h. The molar composition of the gel was as follows: Si/Al = 40, TEAOH/Si = 0.3, surfactant/Si = 0.45, and water/Si = 60. The crystallization was performed at 120 °C for 8 days using a Teflon-lined autoclave. After the second, fourth, and sixth day, pH was adjusted at 10.8 using CH_3COOH (10 wt.%, aqueous). The final solid reaction product was extracted from the autoclave, filtered, washed with distilled water, and dried at 120 °C overnight. Finally, the solid was calcined at 540 °C for 6 h (heating rate 1 °C/min.).

For SBA-15 synthesis, 20 g of amphiphilic triblock copolymer, poly(ethylene glycol)-block-poly(propylene glycol)-block-poly(ethylene glycol) (average molecular weight 5800, Aldrich), was dispersed in 150 g of water and 600 mL of 2 M HCl solution while stirring, followed by the addition of 42 g of tetraethyl orthosilicate to the homogeneous solution with stirring. This gel mixture was continuously stirred at 40 °C for 6 h, and finally crystallized in a Teflon-lined autoclave at 90 °C for 3 days. After crystallization, the solid product was filtered, washed with deionized water, and dried in air at room temperature. The material was calcined in static air at 550 °C for 24 h to decompose the triblock copolymer and obtain a white powder (SBA-15) [48]. This white powder is used as the parent material to produce aluminum-containing material denoted as Al-SBA-15.

Silica SBA-15 (10 g, 166.5 mmol Si) was dispersed in 250 mL of dry hexane containing 0.85 g (4.1 mmol Al) aluminum isopropoxide. The resulting suspension was stirred at room temperature for 24 h, and afterwards the powder was filtered, washed with dry hexane, and dried at 120 °C in air. This solid Al-SBA-15 was then calcined in static air at 550 °C for 6 h (heating rate 1 °C/min) [49].

2.2. Preparation and immobilization of the rhodium diphosphine complexes

In a Schlenk tube under Ar, $[(COD)_2Rh]OTf$ (0.150 mmol) was dissolved in 20 mL of CH_2Cl_2, and then a solution containing the corresponding diphosphine (0.165 mmol diphosphine; *(R,R)-Me-BPE* or *(R,R)-Me-DUPHOS*) was added. The resulting mixture was stirred at room temperature for 6 h, and then the solvent was eliminated under reduced pressure. The obtained solid was dried under vacuum and at 50 °C overnight (see Fig. 1).

In order to immobilize Rh–diphosphine-complexes, 1 g mesostructured material (Al-MCM-41, Al-MCM-48, or Al-SBA-15) was suspended in 9 mL CH_2Cl_2 and stirred at room temperature for 1 h. The Rh–diphosphine-complex (0.15 mmol) was dissolved in 1 mL CH_2Cl_2 and added to the solid/CH_2Cl_2 suspension. The reaction mixture was stirred at room temperature for 24 h followed by solvent evaporation under reduced pressure. The recovered solid was Soxhlet extracted with MeOH for 24 h, in order to remove any residual free Rh-complex (see Fig. 2). The absence of the homogeneous complex in the upper aliquot was checked by ICP-

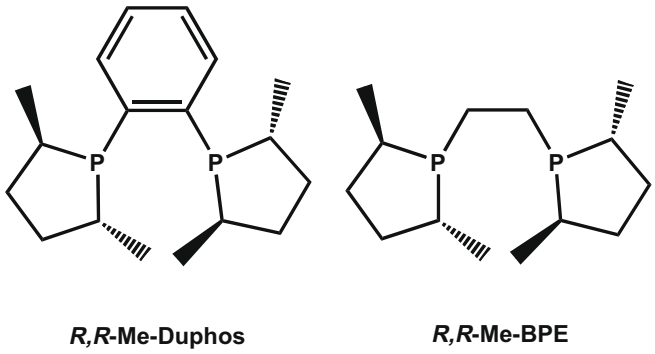

Fig. 1. Diphosphine ligands used in the present study.

AES analysis as well as by FT-IR spectroscopy. The final material was vacuum dried at room temperature overnight.

2.3. Catalyst characterization

XRD powder diffraction patterns were collected on a Siemens Diffractometer D5000 equipped with a secondary monochromator, a variable diaphragm V 20, and a nickel filter using Cu K_α radiation (wavelength 1.5406 Å), the angle speed was 0.02° min^{-1}. Bulk elemental chemical analyses were done with inductive couple plasma atomic emission spectroscopy (ICP-AES) on a Spectroflame D (Spectro Analytic Instrument). Nitrogen adsorption/desorption isotherms at liquid nitrogen temperature were measured on a Micromeritics ASAP 2010 instrument. The samples were pre-outgassed at 150 °C. Pore diameter and specific pore volume were calculated based on the Barrett–Joyner–Halenda (BJH) theory. The specific surface area was obtained using the Brunauer–Emmett–Teller (BET) equation.

FT-IR analyses were done on a Nicolet Protégé 460 equipped with an evacuable furnace cell with KBr windows containing the sample wafer. Without using a binder, the samples were pressed into self-supporting wafers, which, after being mounted onto the sample cell, were dried at 160 °C and 10^{-3} mbar for 16 h.

For thermogravimetric analysis, a Netzsch 209/2/E equipped with a STA 409 controller was used. The heating rate was 5 °C/min, and α-Al_2O_3 was used as a reference material.

2.4. α-1-Arylalkylenamides synthesis

All enamides were synthesized according to a slightly altered method reported by Burk et al. [6]. To argon flushed 2-necked round-bottomed flask, the Grignard reagent (1.3 equivalents; i.e., methyl magnesium iodide, ethyl magnesium iodide, and isopropyl magnesium iodide) in diethyl ether was added. The arylnitrile (30 mmol; i.e., benzonitrile, 4-methylbenzonitrile, 4-trifluoromethylbenzonitrile, 4-methoxybenzonitrile, 4-fluorobenzonitrile, 4-chlorobenzonitrile, and 2-methylbenzonitrile) was added dropwise to the round-bottomed flask, and then the solution was allowed to stir until solidified. The obtained solid was crushed with a spatula. Then, the system was cooled down with the help of dry ice/isopropanol bath, and acetic anhydride (2 equivalents) was added and the mixture was stirred for 1 h. Further, THF was added, and the mixture was allowed to warm at the room temperature under vigorous stirring. The slow addition of excess methanol was followed. The solution was transferred to a separatory funnel, water was added, and then the aqueous mix was extracted three times with chloroform. The organic layers were dried with sodium sulfate and removed under reduced pressure. The crude compound was purified via flash chromatography with an appropriate mixture of hexanes and ethyl acetate as eluent (usually ethyl acetate/hexane = 2/1). The overall yields were usually low, between 5% and 20%. Characterization data of the synthesized molecules were close to the ones reported in the literature.

2.5. Catalytic tests

2.5.1. Homogeneous hydrogenations

In a glove box, a Fischer–Porter bottle was charged with the corresponding amount of substrate, anhydrous, degassed MeOH, and the rhodium diphosphine complex (0.2 mol%). After five vacuum/H_2 cycles, the tube was pressurized to a pressure of 3 bar H_2. The solution was stirred at 20–25 °C for 16 h. The products of reaction were concentrated on a rotavap, and the residue was passed through a short SiO_2 column (EtOAc/hexane: 1/1) to remove the catalyst. Without further purification, the enantiomeric excesses were determined directly on an aliquot of the crude products thus obtained.

2.5.2. Heterogeneous hydrogenations

In a glove box, a Fischer–Porter bottle was charged with the corresponding amounts of substrate, anhydrous, degassed MeOH, and immobilized rhodium disphosphine complex. After five vacuum/H_2 cycles, the tube was pressurized to a pressure of 3 bar H_2. The reactions were allowed to stir at room temperature for 16 h. The aliquots were passed through a 20-μm PTFE filter and submitted to the analysis without any further treatment. Conversion and selectivity were monitored via HPLC (column: RP 18 400 mm), whereas enantioselectivity was determined via a chiral capillary GC using the appropriate chiral column (Chirasil-Dex-CB 25 m or Lipodex G-6).

2.5.3. Recycling

The heterogeneous catalysts were recycled using standard methods (the catalysts were recovered by filtration or centrifugation, washed with 5 mL MeOH, dried overnight under vacuum at room temperature, and reused in the next cycle at the same substrate/catalyst ratio). In order to prove that the reaction was heterogeneously catalyzed and to exclude the possibility of leaching and homogeneous catalysis, the hot filtration test was performed according to Lempers and Sheldon [50].

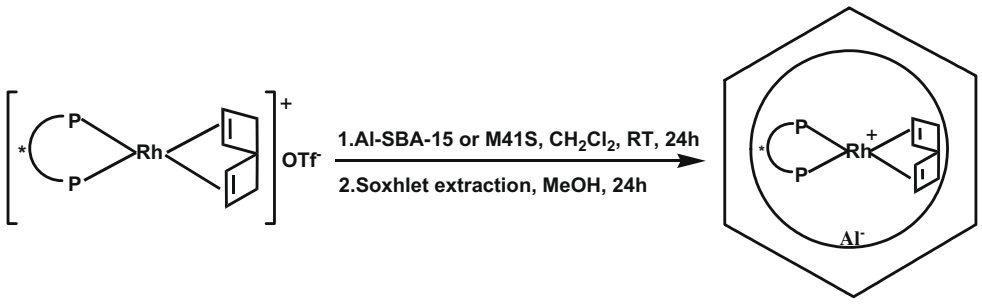

Fig. 2. Immobilization of chiral rhodium complex.

Table 1
Elemental analysis for parent and loaded materials.

Sample	Si mmol/g	Al mmol/g	Na mmol/g	Rh mmol/g	Si/Al	Al/Na	Al/Rh
Al-MCM-41	14.52	0.383	0.386	–	37.90	0.99	–
RhDUPHOS/Al-MCM-41	13.74	0.361	0.301	0.07	38.16	1.19	5.14
Al-MCM-48	14.70	0.396	0.404	–	37.12	0.98	–
RhDUPHOS/Al-MCM-48	13.96	0.368	0.308	0.08	37.93	1.19	4.81

Table 2
Dependence of the Rh content in case of CODRhDUPHOS immobilized on Al-MCM-41 with different Si/Al ratios.

Sample	Si/Al	Rh Mmol/g	Theoretical Rh mmol/g
RhDUPHOS/Al-MCM-41	80	0.02	0.15
RhDUPHOS/Al-MCM-41	40	0.07	0.15
RhDUPHOS/Al-MCM-41	20	0.10	0.15

3. Results and discussion

The X-ray powder diffraction of the Al-MCM-41, Al-SBA-15, and Al-MCM-48 showed the characteristic hexagonal or cubic structure, respectively. Al-MCM-41 showed a sharp peak ascribed to (100) reflection of the hexagonal structure of mesopores at $2\theta = 2.44°$, corresponding to $d_{100} = 3.045$ nm. Besides the strong peak, weak ones ascribed to (110) and (200) reflections at $2\theta = 4.2°$ and 4.9°, $d = 1.68$ and 1.48 nm, respectively, were observed. XRD pattern of Al-MCM-48 sample revealed the presence of a sharp peak ascribed to the (211) reflection of the cubic structure at $2\theta = 2.28°$, corresponding to $d_{211} = 3.327$ nm. A second peak corresponding to the (220) reflection was observed at $2\theta = 2.76°$. Al-SBA-15 showed a well-resolved pattern with a prominent peak at 0.8°, and two peaks at 1.4° and 1.6° 2θ which match well with the pattern reported for SBA-15 [51]. The XRD peaks can be indexed to a hexagonal lattice with a $d_{(100)}$ spacing of 110 Å, corresponding to a large unit cell parameter $a_0 = 127$ Å ($a_0 = 2d(100)/\sqrt{3}$). However, for carrier materials the intensity of the reflections essentially did not change upon loading the carrier with the organometallic complexes, nor after a catalytic cycle, showing that the mesoporous structures were not affected by the incorporation of the catalyst.

The elemental analysis showed a Rh content between 0.07 and 0.08 mmol/g, whereas the theoretical content was 0.15 mmol/g (Table 1). The color transfer from the transition metal complex solution to the white solid during the first immobilization step showed a complete immobilization of the complex onto the solid surface. For this step, the impregnation solvent of choice was anhydrous dichloromethane because of its aprotic nature and its capability to dissolve appreciable amounts of complex. Alcohols cannot be used as they compete with the Rh complexes for interaction with the solid surface. Upon extraction with methanol, the second immobilization step, which in contrast to the nonpolar dichloromethane, adsorbs strongly on the carrier surface, the organometallic complex desorbs from the terminal silanol groups due to a competitive reaction with the polar alcohol.

The dependence of the immobilization on the aluminum content of the mesoporous materials was studied in case of Al-MCM-41 by using materials with Si/Al ratios of 20, 40 and 80 (Table 2). These complementary experiments showed an almost linear dependence of the immobilized rhodium with the aluminum content of Al-MCM-41. The attempt to immobilize the complexes on all silica M41S and SBA-15 failed due to a complete removal of the complex from the solid surface during the Soxhlet extraction. These results clearly showed the influence of the network tetrahedral aluminum. This tetrahedral aluminum is negatively charged, and a counter cation is present for charge neutralization. In case of Al-MCM-41 and Al-MCM-48, the negative charge is neutralized by a sodium cation. Table 1 presents the aluminum/sodium molar ratio before and after immobilization. As expected, after immobilization this ratio is increasing due to the ionic exchange of sodium with the cationic rhodium complex.

N_2 sorption isotherms were measured for the pure carrier and for all immobilized complexes, respectively. Fig. 3 and Table 3 present a comparison of sorption isotherms and textural characteristics for pure and loaded samples. In all the cases, these isotherms presented the characteristic form of mesoporous materials. It can be easily remarked that the N_2-adsorbed/desorbed volume was higher in the case of pure carrier than in the case of immobilized complexes.

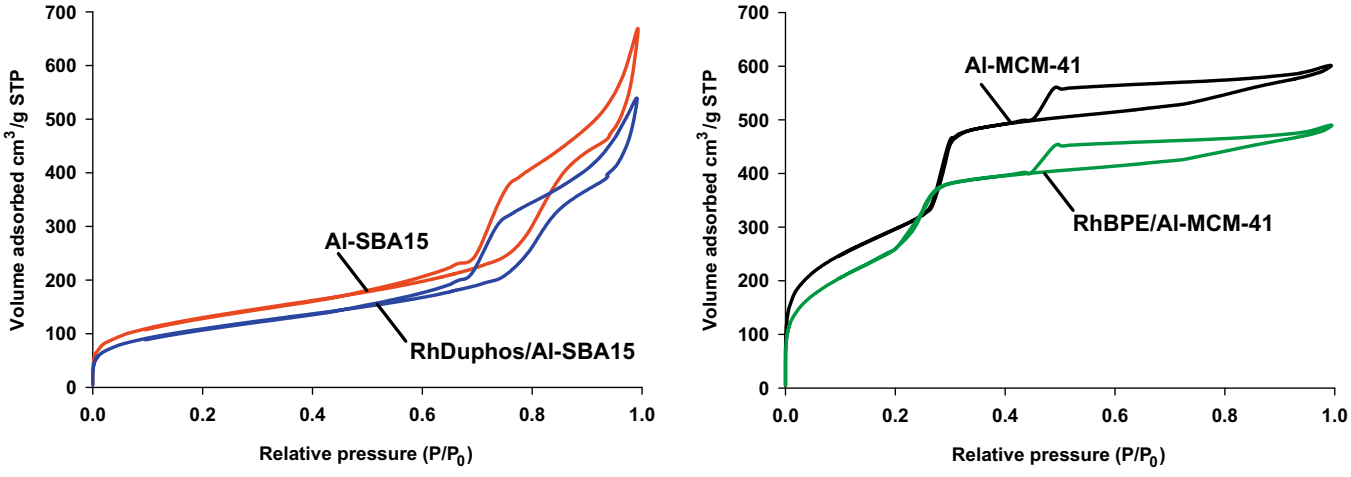

Fig. 3. N_2 sorption isotherms.

Table 3
Textural characteristics of parent and loaded materials.

Sample	Surface area ($m^2\ g^{-1}$)	Pore volume ($cm^3\ g^{-1}$)	Pore diameter (Å)
Al-MCM-41	1190	0.97	34
RhDUPHOS/Al-MCM-41	1092	0.77	29
Al-SBA-15	467	0.92	94
RhDUPHOS/Al-SBA-15	397	0.78	89

The infrared spectra of the loaded materials revealed the presence of bands attributable to the characteristic organic structure of the diphosphine complexes. Although these bands are weak and not characteristic enough to resolve a structure, several typical bands could be distinguished, as for example the =C–H band centered at 2962 cm^{-1} and 2857 cm^{-1}. Furthermore, a medium strength band at 1460 cm^{-1} was found, which could be assigned to the CH_2 bending vibration or P–C–H group (see Fig. 4).

The acidity of the samples was characterized by FTIR spectroscopy investigating the spectra of adsorbed pyridine as probe molecule. The spectra of adsorbed pyridine (Py) after degassing at 200 °C are presented in Fig. 5. Pure silica materials have an electrically neutral framework and consequently showed no Lewis or Brønsted acidity. After incorporation of aluminum, the FTIR spectra of adsorbed Py showed that both Lewis and Brønsted acid sites were created. Al-MCM-41, Al-MCM-48 and Al-SBA-15 exhibited several peaks due to strong Lewis-bound pyridine (1623 cm^{-1} and 1456 cm^{-1}), weak Lewis-bound pyridine (1577 cm^{-1}), and pyridinium ion on Brønsted acid sites (1546 cm^{-1} and 1641 cm^{-1}), while all silica SBA-15 showed only small peaks due to hydrogen-bonded pyridine (1446 cm^{-1} and 1596 cm^{-1}) [52,53]. Moreover, after the immobilization of the organometallic complex a slight decrease in the Brønsted and Lewis acidity was observed. This decrease is due to guest/host interaction between the organometallic complex and the solid framework.

Temperature-programed desorption of ammonia was used to characterize the acidity of all silica and aluminated SBA-15, as well as Al-MCM-41 and Al-MCM-48. Fig. 6 presents the results obtained for SBA-15 and Al-SBA-15. Comparison of these TPD curves showed an increase of the total acidity after alumination. The peaks with maxima at about 300 °C, found for both samples, were due to weakly bonded ammonia (physisorbed ammonia and ammonia adsorbed on weak acid sites). The peaks centered at 480 °C were not well defined, and an interpretation could be risky. These experiments showed that weak acid sites were formed after alumination on the surface of the solid.

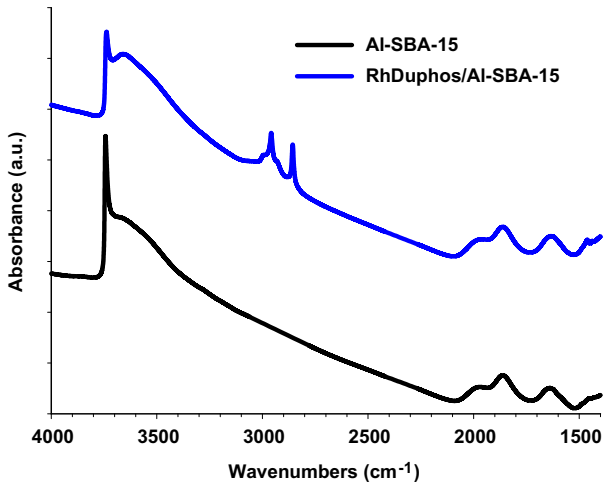

Fig. 4. IR spectra of Al-SBA-15 and RhDuphos/Al-SBA-15.

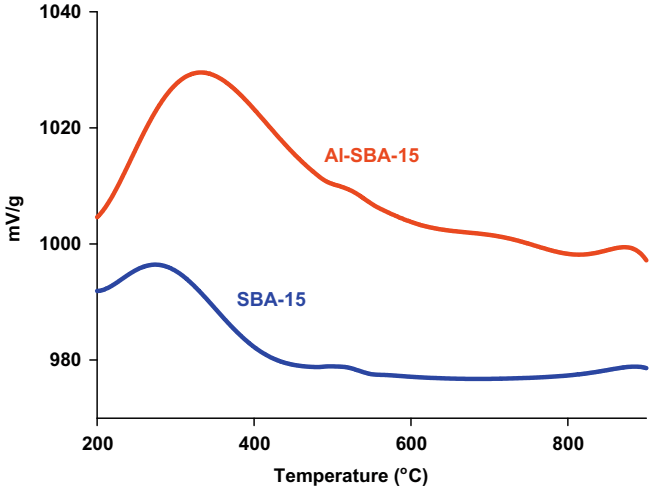

Fig. 6. Temperature-programed desorption of ammonia of SBA-15 and Al-SBA-15.

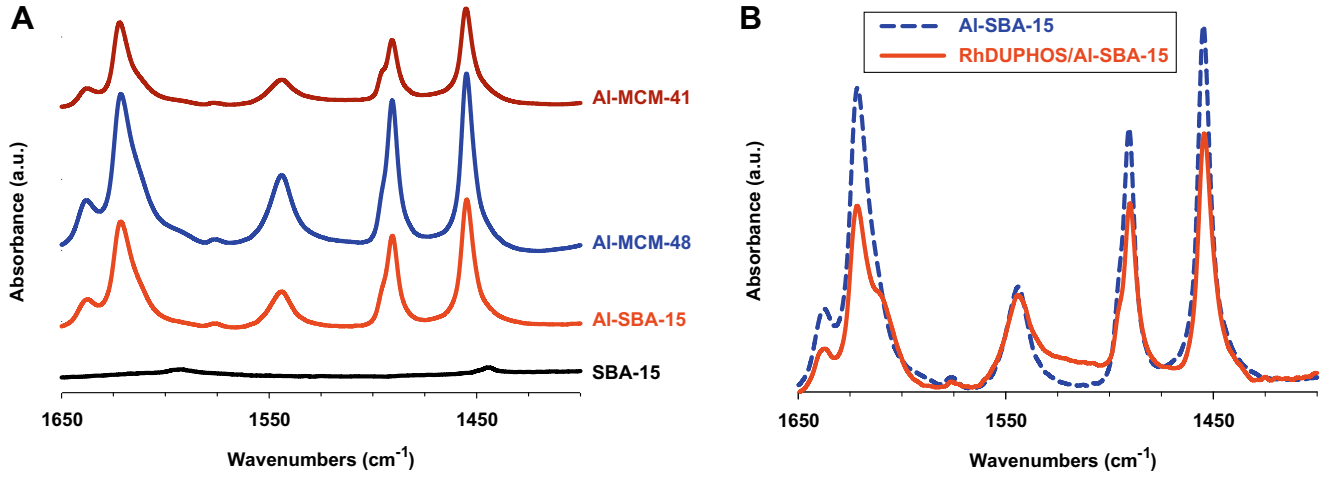

Fig. 5. IR spectra of adsorbed pyridine: (A) pure carriers and (B) Al-SBA-15 and RhDUPHOS/Al-SBA-15.

For Al-MCM-41, temperature-programed desorption of ammonia showed the presence of weak acidic centers on this type of carrier material. In the case of the immobilized complex, the amount of desorbed ammonia decreases compared to the pure carrier material (Fig. 7). This indicates an interaction of the immobilized complex with acidic sites on the Al-MCM-41. This result was also supported by FT-IR spectroscopy.

Quantitative loading of the organometallic complex on the considered supports was demonstrated with thermogravimetric analyses. For all the immobilized complexes, thermogravimetric and differential scanning calorimetric measurements showed a thermal stability up to 200 °C. In general, the loss of weight for the heterogenized catalysts as a function of temperature was about 3–5 wt%. Since the oxidation of the pure carriers showed no characteristic peak, we attribute the weight loss to the decomposition of the Rh-complex. The results were consistent with the Rh and P content determined by ICP AES analyses. For all studied samples, the oxidation of the organic groups took place in two steps, corresponding in DSC spectra to two peaks with maxima at about 250 or 400 °C. Fig. 8 evidences these observations on the example of RhBPE/Al-SBA-15.

In order to elucidate the chemical structure of the immobilized rhodium diphosphine complexes, MAS-NMR of the pure Al-SBA-15 carrier, the homogeneous complexes, and the immobilized complexes have been recorded. Due to the low content of the immobilized complex, the ^{13}C and ^{1}H resonance signals were too weak for quantitative interpretation. The pure carrier and immobilized complexes showed not significantly different spectra for the ^{27}Al and ^{29}Si nuclei. Therefore, the interpretation of a chemical shift is risky.

^{31}P MAS NMR spectra of the solid homogeneous CODRhDuhos complex and the same complex immobilized on Al-MCM-41 were recorded (Fig. 9). The homogeneous complex gave a strong signal at 68 ppm. The MAS NMR spectrum of the immobilized CODRhDUPHOS complex showed only a single signal at 90 ppm. The absence of signals of the homogeneous complex and of the free phosphine ligand was an indication that the phosphine ligand was completely coordinated to the rhodium. Similar results were obtained for CODRhDUPHOS immobilized on Al-MCM-48 or Al-SBA-15. The immobilization of this rhodium DUPHOS complex led to a shift of the ^{31}P signal of 22 ppm to lower magnetic field compared to that of the homogeneous complex as a result of the interaction of the guest complex with the surface of the Al-MCM-41 host, more specifically to the interaction with a Lewis acidic center on the surface

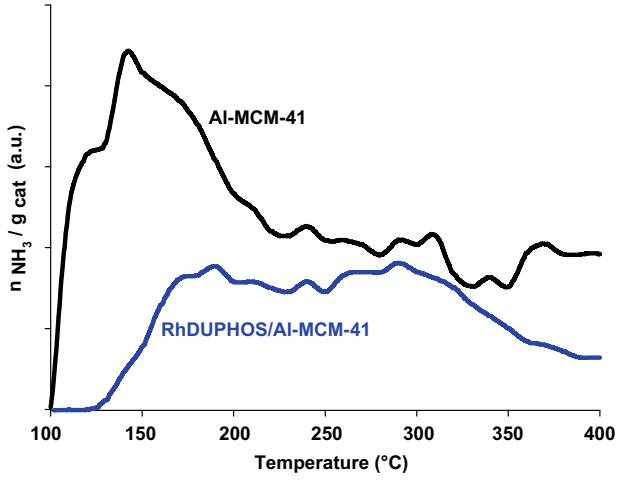

Fig. 7. Temperature-programed desorption of ammonia of Al-MCM-41 and RhDUPHOS/Al-MCM-41.

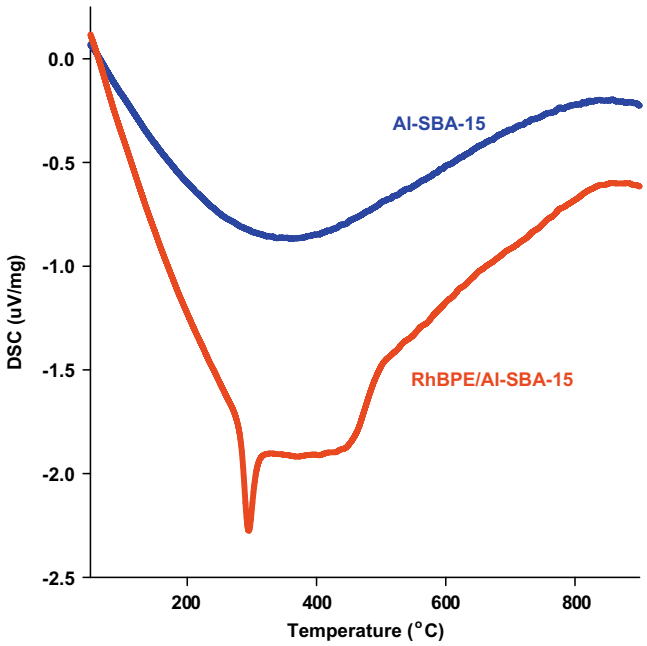

Fig. 8. DSC spectra of Al-SBA-15 and RhBPE/Al-SBA-15.

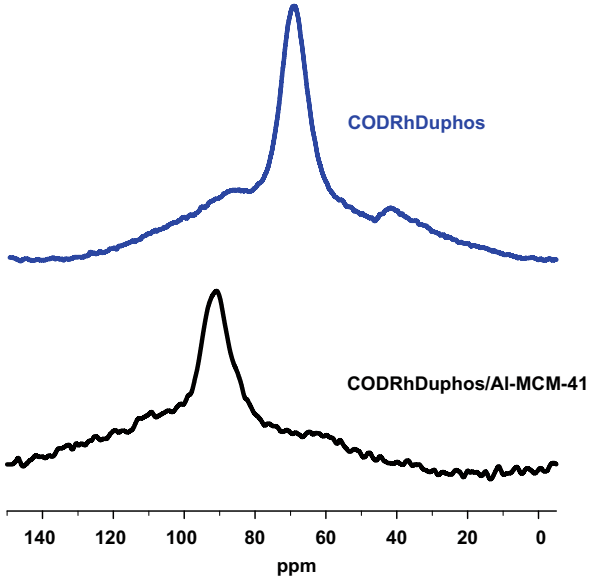

Fig. 9. ^{31}P MAS NMR of homogeneous CODRhDuphos and CODRhDuphos immobilized on Al-MCM-41.

which withdraws electrons from the rhodium metal or the phosphine ligand, and thus lowers the electron density.

The rhodium complexes used consisted of a chiral diphosphine and a cyclooctadiene ligand. There could be several forces involved in the bonding of the complex to aluminum-containing mesostructured materials. For example, an electrostatic interaction of the cationic complexes with the anionic framework of the mesoporous material could occur. A similar mechanism was reported for the immobilization of manganese complexes on Al-MCM-41 [54]. Furthermore, direct bridging of the rhodium to surface oxygen of the mesoporous walls has also been observed and could occur after cleavage of the diene complex during the hydrogenation reaction [55]. However, no evolution of cyclooctadiene during the immobilization reaction could be observed, and FT-IR spectra of the filtrate

obtained after the impregnation did not contain bands attributable to free cyclooctadiene.

3.1. Catalytic results

[(COD)RhDUPHOS]OTf and [(COD)RhBPE]OTf have been tested for immobilization on aluminum-containing mesoporous materials. The activity of the free and immobilized complexes in enantioselective hydrogenation of different α-1-arylalkylenamides synthesis was investigated (Fig. 10). In blank reactions using the parent materials, no reactions took place, and over Rh supported on mesostructured materials no enantiomeric excess was observed, although conversions up to 99% percent were found. Moreover, for all hydrogenation experiments the chemical selectivity was >99%. No side products were observed.

As presented in Table 4, the enantioselectivities obtained in the presence of heterogenized RhBPE complex were with maximal 5% lower than the ones obtained over the free complex. For heterogeneous catalysis, the reaction rates were higher for Al-MCM-48-based catalyst. However, the reaction rates were higher for homogeneously performed reactions. Substitution at para position did not greatly influence the enantioselectivity. No significant electronic effects on the enantioselectivity were observed. However, it was found that substitution at the ortho-position has a big effect both on the activity and on the enantioselectivity. For example, hydrogenation of *N*-acetyl-1-(2′-methylphenyl) etheneamine over RhBPE/Al-MCM-41 occurred with 49% conversion and 55.4% e.e.

Table 5 presents the best results obtained with free and immobilized RhDUPHOS complexes. In all cases, the enantioselectivity obtained over the immobilized RhDUPHOS complex was slightly lower compared to that obtained over the free complexes. The enantioselectivity obtained in the hydrogenation of *N*-acetyl-1-phenyletheneamine over RhDUPHOS was of 95.3 for the immobilized complex and of 95.8% for the free complex, respectively. Moreover, turn over frequency corresponding to the first hour of reaction was lower in case of immobilized RhDUPHOS complex. For example, the corresponding $TOF_{FIRST\ HOUR}$ obtained for the hydrogenation of *N*-acetyl-1-phenyletheneamine was 268 h^{-1} for the immobilized complex and was 379 h^{-1} for the free complex, respectively. However, the hydrogenation of α-arylenamides over immobilized RhDUPHOS occurred with more than 94% conversion and 95.3% enantioselectivity.

The dependence of reaction speed and enantioselectivity with the reaction temperature was investigated. As expected, the hydrogenation of α-arylenamides at higher temperatures was performed faster but with slightly lower enantioselectivities. For example, hydrogenation of *N*-acetyl-1-phenyletheneamine over RhBPE/Al-MCM-41 occurred with 94.3 or 92.4% e.e. at 45 or 60 °C, with corresponding $TOF_{FIRST\ HOUR}$ of 311 or 405 h^{-1} respectively. Moreover, it was found that hydrogenation of such substrates both over free and heterogenized RhBPE complex is less sensitive to the solvent. By use of different solvents such as MeOH, EtOH, i-PrOH, CH_2Cl_2, THF, EtOAc, and toluene, the enantioselectivity varied with <5%. However, the reaction rates were slightly lower when aprotic solvent is used.

Table 4
Hydrogenation of α-arylenamides over free or immobilized RhBPE complex.[a]

Entry	R	Support	Conversion[b] (%)	e.e.[c] (%)	$TOF_{FIRST\ HOUR}$[d] (h^{-1})
1[e]	H	–	>99	96.9	412
2	H	Al-MCM-41	99	95.6	247
3	H	Al-MCM-48	99	96.4	280
4	H	Al-SBA-15	99	91.6	219
5[e]	CH_3	–	>99	97.2	384
6	CH_3	Al-MCM-41	99	95.6	298
7	CH_3	Al-MCM-48	99	96.8	345
8	CH_3	Al-SBA-15	94	94.4	244
9[e]	CF_3	–	>99	99.0	n.d.
10	CF_3	Al-MCM-41	92	97.1	n.d.
11	CF_3	Al-MCM-48	99	99.0	n.d.
12	CF_3	Al-SBA-15	86	97.3	n.d.
13[e]	F	–	>99	97.8	405
14	F	Al-MCM-41	99	97.3	256
15	F	Al-MCM-48	99	97.8	321
16	F	Al-SBA-15	98	97.5	128
17[e]	Cl	–	>99	97.9	395
18	Cl	Al-MCM-41	99	95.4	357
19	Cl	Al-MCM-48	99	96.2	372
20	Cl	Al-SBA-15	99	95.9	320
21[e]	OCH_3	–	>99	96.8	n.d.
22	OCH_3	Al-MCM-41	96	95.3	n.d.
23	OCH_3	Al-MCM-48	99	95.9	n.d.
24	OCH_3	Al-SBA-15	91	94.8	n.d.

[a] All reactions were conducted at room temperature and a H_2 pressure of 3 bar, using 0.05–0.1 M solutions of substrate and a S/C ratio of 500. Reaction time was 16 h, and >99% chemoselectivity was observed in all cases.
[b] The catalytic activity was monitored by HPLC.
[c] Enantiomeric excesses were determined chiral capillary GC using Chromopack Chirasil column.
[d] Turn over frequency measured at a reaction time of 1 h.
[e] Reaction performed in the presence of [CODRhBPE]OTf.

Table 5
Hydrogenation of α-arylenamides over free or immobilized RhDUPHOS complex.[a]

Entry	R	Support	Conversion[b] (%)	e.e.[c] (%)	$TOF_{FIRST\ HOUR}$[d] (h^{-1})
1[e]	H	–	>99	95.8	379
2	H	Al-SBA-15	99	95.3	268
3[e]	CH_3	–	>99	96.2	397
4	CH_3	Al-MCM-48	96	96.0	271
5[e]	F	–	>99	98.0	365
6	F	Al-MCM-48	98	97.1	244
7[e]	Cl	–	>99	98.7	401
8	Cl	Al-MCM-41	98	98.1	288
9[e]	OCH_3	–	>99	97.3	n.d.
10	OCH_3	Al-MCM-41	94	96.9	n.d.

[a] All reactions were conducted at room temperature and a H_2 pressure of 3 bar, using 0.05–0.1 M solutions of substrate and a S/C ratio of 500. Reaction time was 16 h and >99% chemoselectivity was observed in all cases.
[b] The catalytic activity was monitored by HPLC.
[c] Enantiomeric excesses were determined via a chiral capillary GC using Chromopack Chirasil column.
[d] Turn over frequency measured at a reaction time of 1 h.
[e] Reaction was performed in the presence of [CODRhDUPHOS]OTf.

It was also examined whether the heterogenized catalysts could effectively hydrogenate α-arylenamides possessing β-substituents

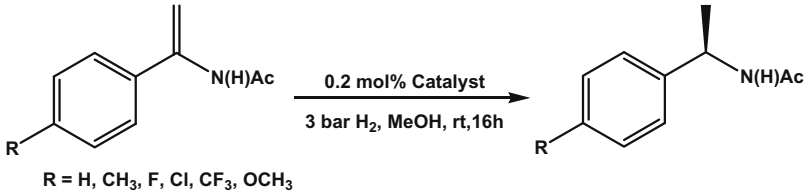

Fig. 10. Hydrogenation of α-arylenamides.

(i.e., *N*-acetyl-1-phenylpropeneamine and *N*-acetyl-1-(4′-trifluoromethylphenyl)isobuteneamine; Fig. 11). Although e.e. higher than 95% was obtained for hydrogenation of such substrates over RhBPE/Al-MCM-48, complete conversions were obtained only for low substrate/catalyst ratios (S/C = 100). No investigation of the substrates E/Z issues and their influence on catalytic activity was carried out.

The recyclability of the immobilized rhodium diphosphine complexes was tested using standard procedures. It was found that these catalysts could be recycled four times without any loss of activity and chemo- or enantioselectivity. Fig. 12 presents the reuse of RhBPE/Al-MCM-48 in hydrogenation of *N*-acetyl-1-phenyletheneamine at S/C ratio of 500. For this reaction, turn over number over the 4 cycles was >2000. Moreover, only 89% conversion was obtained for the hydrogenation of *N*-acetyl-1-phenyletheneamine over homogeneous RhBPE at S/C ratio of 1000, which corresponds to a TON of 890. This fact demonstrates that by recycling the immobilized catalyst the overall TON of the reaction can be increased.

In order to prove that the reaction is catalyzed heterogeneously and to exclude the possibility of leaching and homogeneous catalysis, the reaction mixture was separated from the catalyst before complete conversion occurred (hot filtration test) [49]. In the case of hydrogenation of *N*-acetyl-1-phenyletheneamine over RhBPE/Al-MCM-48, no further reaction was found after filtration at 1 h (Fig. 12). After 16 h, the conversion of the filtered sample remains at 43%, whereas the original batch with catalyst was completely converted. This test proved that no homogeneous catalysis took place.

The deprotection of the amine group has not been investigated. However, the literature reports showed that the synthesized amides could be hydrolyzed using well-known methods to the corresponding amines without loss of chirality [6,7]. According to the above-mentioned reports, no racemization was observed during deprotection step.

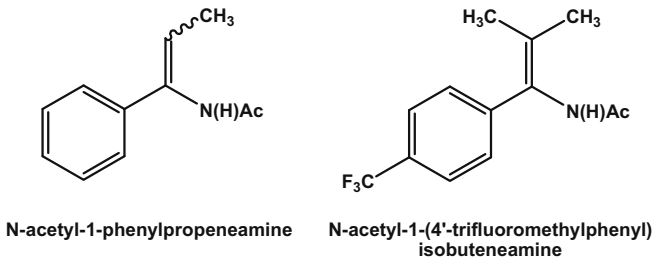

Fig. 11. β-substituted α-arylenamides.

4. Conclusion

Heterogeneous chiral catalysts were prepared from chiral rhodium diphosphine complexes and aluminum-containing MCM-41, MCM-48, and SBA-15. The complexes were bonded to the carrier by the interaction of the cationic rhodium of the organometallic complex with the anionic host framework, as well as between Al Lewis acid sites and P Lewis basic sites. This method is effective and simpler than covalent bonding of guest molecules.

These heterogenized catalysts were applied for asymmetric hydrogenation of α-arylenamides. The immobilized catalysts showed high activities and excellent chemo- and enantioselectivities, achieving up to 99% e.e. at 99% conversion and >99% selectivity. To the best of our knowledge, it is for the first time α-1-arylalkylamines derivatives are obtained with the help of asymmetric heterogeneous catalysis.

The recyclability of rhodium diphosphine complexes immobilized on aluminum-containing mesostructured materials was demonstrated using standard procedures. The catalysts could be reused at least four times without any activity loss, obtaining TON larger than 2000. The high activities observed with these supported organometallic complexes, plus the fact that the high activity is maintained upon reuse of the catalysts, indicated that these are truly heterogeneous counterparts of homogeneous transition metal complexes.

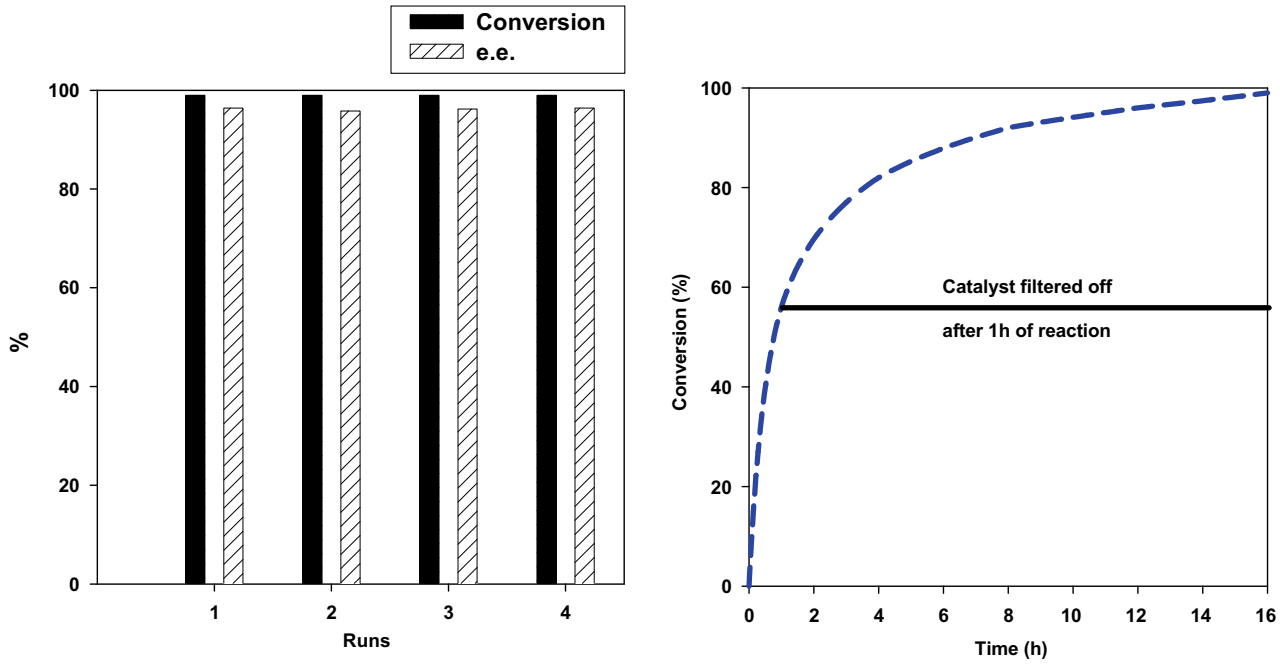

Fig. 12. Recycling and hot filtration test for hydrogenation of *N*-acetyl-1-phenyletheneamine over RhBPE/Al-MCM-48.

Acknowledgment

The authors are very grateful for the financial support from the Sonderforschungsbereich SFB 380 of the Deutsche Forschungsgemeinschaft (DFG).

References

[1] J. Jacques, A. Collet, S.H. Wilen, Enantiomers, Racemates, and Resolutions, John Wiley and Sons, New York, 1981.
[2] M. Nogradi, Stereoselective Synthesis, second ed., VCH, Weinheim, 1995.
[3] S. Itsuno, M. Sasaki, S. Kuroda, K. Ito, Tetrahedron: Asymmetry 6 (1995) 1507.
[4] M.M. Gharpure, A.S. Rao, Synthesis (1988) 410.
[5] D. Rossi, A. Calcagni, A. Romeo, J. Org. Chem. 44 (1979) 2222.
[6] M.J. Burk, Y. Wang, J. Lee, J. Am. Chem. Soc. 118 (1996) 5142.
[7] M. van den Berg, R.M. Haak, A.J. Minnaard, A.H.M. de Vries, J.G. de Vries, B.L. Feringa, Adv. Syn. Catal. (2003) 1003.
[8] W.S. Knowless, Angew. Chem., Int. Ed. 41 (2002) 1998.
[9] R. Noyori, Angew. Chem., Int. Ed. 41 (2002) 2008.
[10] K.B. Sharpless, Angew. Chem., Int. Ed. 41 (2002) 2024.
[11] H.U. Blaser, E. Schmidt, Asymmetric Catalysis on Industrial Scale, Wiley, 2003.
[12] K. Mikami, M. Lautens, New Frontiers in Asymmetric Catalysis, Willey, 2007.
[13] R.A. Sheldon, Curr. Opin. Solid State Mater. Sci. 1 (1996) 101.
[14] B. Pugin, H.U. Blaser, Comprehensive asymmetric catalysis, in: E.N. Jacobsen, A. Pfaltz, H. Yamamoto (Eds.), Springer, Berlin, Heidelberg, New York, 1999.
[15] H.U. Blaser, B. Pugin, M. Studer, Chiral catalyst immobilization and recycling, in: I.F.J. Vankelecom, D.E. De Vos, P.A. Jacobs (Eds.), Wiley-VCH, Weinheim, 2000.
[16] F.J. Waller, Chem. Ind. 89 (2003) 1.
[17] R. Arshady, Microspheres Microcapsules Liposomes 1 (1999) 197.
[18] D. Bergbreiter, Chiral catalyst immobilization and recycling, in: I.F.J. Vankelecom, D. De Vos, P.A. Jacobs (Eds.), Wiley-VCH, Weinheim, 2000, p. 43.
[19] D.E. Bergbreiter, Chem. Rev. 102 (2002) 3345.
[20] A.K. Kakkar, Chem. Rev. 102 (2002) 3579.
[21] C.A. Mc Namara, M.J. Dixon, M. Bradley, Chem. Rev. 102 (2002) 3275.
[22] N.E. Leadbeater, M. Marco, Chem. Rev. 102 (2002) 3217.
[23] Q.-H. Fan, Y.-M. Li, A.S.C. Chan, Chem. Rev. 102 (2002) 3385.
[24] R. Van Heerbeek, P.C.J. Kamer, P.W.N.M. Van Leeuwen, J.N.H. Reek, Chem. Rev. 102 (2002) 3717.
[25] M. Benaglia, A. Puglisi, F. Cozzi, Chem. Rev. 103 (2003) 3401.
[26] S. Braese, F. Lauterwasser, R.E. Ziegert, Adv. Syn. Catal. 345 (2003) 869.
[27] T. Frenzel, W. Solodenko, A. Kirschning, Polymeric materials in organic synthesis and catalysis, in: E.R. Buchmeiser (Ed.), Wiley-VCH, Weinheim, 2003, p. 201.
[28] M.H. Valkenberg, W.F. Holderich, Catal. Rev. 44 (2002) 321.
[29] I.F.J. Vankelecom, P.A. Jacobs, Chiral catalyst immobilization and recycling, in: I.F.J. Vankelecom, D. De Vos, P.A. Jacobs (Eds.), Wiley-VCH, Weinheim, 2000, p. 19.
[30] S. Anderson, H. Yang, S.K. Tanielyan, R.L. Augustine. Chem. Ind. 82 (2001) 557.
[31] C.E. Song, S.-G. Le, Chem. Rev. 102 (2002) 3495.
[32] D.E. De Vos, M. Dams, B.F. Sels, P.A. Jacobs, Chem. Rev. 102 (2002) 3615.
[33] D. De Vos, B.F. Sels, P.A. Jacobs, Adv. Catal. 46 (2001) 1.
[34] R. Haag, Angew. Chem., Int. Ed. 41 (2001) 520.
[35] W.F. Hoelderich, H.H. Wagner, M.H. Valkenberg, Roy. Soc. Chem. 266 (2001) 76. Special publication.
[36] R. Augustine, S. Tanielyan, S. Anderson, H. Yang, Chem. Commun. (1999) 1257.
[37] F. M de Rege, D.K. Morita, K.C. Ott, W. Tumas, R.D. Broene, Chem. Commun. (2000) 1797.
[38] D. De Vos, F. Thibault-Starzyk, P.P. Knops-Gerrits, R.F. Parton, P.A. Jacobs. Macromol. Symp. 80 (1994) 157.
[39] J.P. Arhancet, M.E. Davis, J.S. Merola, B.E. Hanson, Nature 339 (1989) 454.
[40] M.E. Davis, Chemtech 22 (1992) 498.
[41] B. Cornils, W.A. Herrmann, Applied Homogeneous Catalysis with Organometallic Compounds, Developments, vol. 2, Wiley-VCH, Weinheim, 2002.
[42] A. Crosman, W.F. Holderich, in: Proceedings of the 14th International Zeolite Conference, Cape Town, South Africa, 2004, p. 2839.
[43] A. Crosman, W.F. Holderich, J. Catal. 232 (2005) 43.
[44] A. Crosman, W.F. Hoelderich, Catal. Today 121 (2007) 130.
[45] A. Crosman, C. Schuster, H. Wagner, M. Batorfi, J. Cubilos, W.F. Hoelderich, in: D. Enders, K.-E. Jaeger (Eds.), Asymmetric Synthesis with Chemical and Biological Methods, WILEY-VCH Verlag, Weinheim, 2007, p. 277.
[46] W.P. Hems, P. McMorn, S. Riddel, S. Watson, F.E. Hancock, G.J. Hutchings, Org. Biomol. Chem. 3 (2005) 1547.
[47] J.H.C. van Hooff, Micropor. Mater. 5 (1995) 211.
[48] D. Zhao, J. Am. Chem. Soc. 120 (1998) 6024.
[49] Z. Luan, Chem. Mater. 11 (1999) 1621.
[50] H.E.B. Lempers, R.A. Sheldon, J. Catal. 175 (1998) 62.
[51] A. Sayari, B.-H. Han, Y. Yang, J. Am. Chem. Soc. 126 (2004) 14348.
[52] I. Kiricsi, C. Flego, G. Pazzuconi, W.O. Parker Jr., R. Millini, C. Perego, G. Bellussi, J. Phys. Chem. 98 (1994) 4627.
[53] T. Barzetti, E. Selli, D. Moscotti, L. Forni, J. Chem. Soc., Faraday Trans. 92 (1996) 1401.
[54] S.S. Kim, W. Zhang, T.J. Pinnavaia, Catal. Lett. 43 (1997) 149.
[55] A. Janssen, J.P.M. Niederer, W.F. Hölderich, Catal. Lett. 48 (1997) 165.